

PERMANENT MAGNET DC MOTOR SLIDING MODE CONTROL SYSTEM

S. Vaez-Zadeh and M. Zamanian

*Advanced Motion Systems Research Laboratory, Department of Electrical and Computer Engineering
University of Tehran, North Kargar Ave., P. O. BOX 14395/515
Tehran, Iran, Fax +(98) 21 877-8690, vaezs@ut.ac.ir*

(Received: August 6, 2002 – Accepted in Revised Form: September 16, 2003)

Abstract In this paper a sliding mode controller (SMC) is designed for a permanent magnet direct current (PMDC) motor to enhance the motor performance in the presence of unwanted uncertainties. Both the electrical and mechanical signals are used as the inputs to the SMC. The complete motor control system is simulated on a personal computer with different design parameters and desirable system performance is obtained. The experimental implementation of the motor control system by a floating point DSP is also presented. The test results confirm the simulation results and validate the proposed motor control system for high performance applications.

Key Words Permanent Magnet, DC Motor, Sliding Mode Controller, SMC

چکیده در این مقاله یک کنترل کننده مود لغزشی (SMC) طراحی گردیده است تا عملکرد موتور مغناطیس دائم جریان مستقیم (PMDC) را در حضور نا معینیهای ناخواسته بهبود بخشد. هر دو سیگنال الکتریکی (جریان موتور) و مکانیکی (سرعت موتور) به عنوان ورودی SMC استفاده شده اند. سیستم موتور و کنترل کننده توسط یک رایانه شخصی به ازای مقادیر مختلف پارامترهای کنترل کننده شبیه سازی شده که نتایج آزمایشهای انجام شده بر آن، نتایج شبیه سازی را تایید کرده و حاکی از عملکرد مناسب سیستم تحت کنترل می باشد.

1. INTRODUCTION

Permanent Magnet (PM) motors are by far the biggest user of permanent magnet materials capturing 60 percent of the PM market. The explosive rate of growth of PM motor market, exceeding 25% annually in the last decade, not only relied on discovery of high energy PM materials like NdFeB and SmCo, but also is due to the advent of related motor drive technologies. These include high frequency high power semiconductor switches like IGBTs and MOSFETs and microelectronic data processing hardware like microcontrollers and digital signal processors (DSP's) [1]. Also the utilization of modern control strategies has shown a new perspective in the use of PM motors in high performance applications including factory automation, robotics, aerospace, etc [2-10]. In particular the sliding mode control theory has gained considerable attention in motor control systems due to its robustness against load torque disturbances and motor parameter variations [2-8].

SMC of PM motors is traditionally implemented

by using an outer speed control loop with a sliding mode controller and inner current or torque control loop with a linear controller. The use of sliding mode controllers in both speed loop and current loop has been proposed to improve torque response and system robustness [3]. However, the chattering effect, that is inherent in sliding mode control, is elevated due to cascade (serial) allocation of two sliding mode controllers. Recently, an improved cascade sliding mode controller for permanent magnet synchronous machines is presented that produces low chattering [4]. This method needs on-line calculation of control signal. An alternative method is the use of state space sliding mode control. This method has been proposed in different approaches [5-8]. These approaches provide excellent system robustness and performance. However, they usually suffer from the system complexity and rely on the designer experience or trial and error procedures. These drawbacks still can be justified in permanent magnet AC machines. But in a permanent magnet direct current (PMDC) machine, with a linear model, simpler approaches

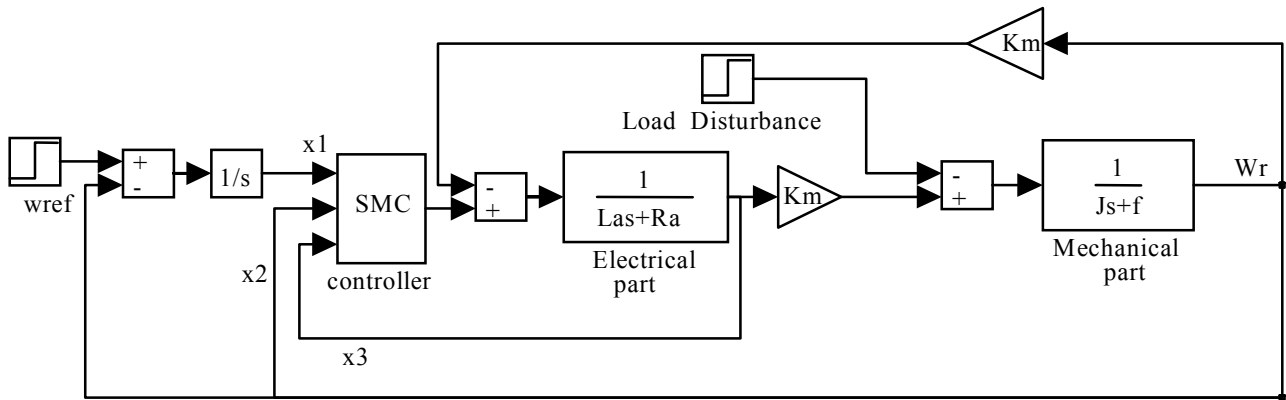


Figure 1. Block diagram of PMDC motor sliding mode control system.

are desirable.

In this paper a sliding mode controller (SMC) is designed for a PMDC motor based on the state space control theory. The design procedure is straightforward and results in closed form solutions for the control parameters. The controller synthesis is directly related to the desired performance specifications.

The complete motor control system including the designed SMC is simulated on a personal computer and the motor performance is evaluated. The SMC provides improved motor performance and robustness over an alternative state feedback controller (SFC) in terms of load disturbance rejection capability and parameter variations. A DSP implementation and experimental evaluation of the motor control system are also presented. The experimental results confirm the simulation results and validate the control system design and implementation.

2. MATHEMATICAL MODEL

The system model including a PMDC motor with a sliding mode control is shown in the block diagram of Figure 1 [2]. The mathematical description of the system in state space is represented by the following state equations:

$$\dot{x} = Ax + Bu + Fw, \quad x(0) = 0$$

$$x = [x_1, x_2, x_3]^T = \left[\int (\omega_{ref} - \omega_r) dt, \omega_r, i_a \right]^T \quad (1)$$

where x is the state vector, with x_1 (integral of speed error), x_2 (ω_r : speed), and x_3 (i_a : motor armature current) as states; u is the control signal; ω_{ref} is the motor speed reference input (speed command), ω_r is speed deviation and T_L is load torque. The motor armature voltage, v_a , is used as the control signal.

System parameters are motor friction coefficient, f ; motor inertia coefficient, J ; motor torque constant, K_m ; armature resistance R_a and armature inductance L_a .

3. SLIDING MODE CONTROLLER

The motor control system behavior in transient condition consists of two modes of operation. One is the reaching mode in which the state trajectory moves from the initial conditions towards the switching surface. The other one is the sliding mode in which the state trajectory slides on the switching surface towards the steady state condition. Therefore, designing the controller consists of two steps; selecting a proper switching surface, and determining an adequate control signal [11]. These are explained here.

3.1 Switching Function The switching function, $S(x)$, is the main factor in forming a sliding mode control system. The controller structure changes according to the sign of this function. By this way the state trajectory remains close to the switching surface in the sliding mode. The switching surface is

where the function is equal to zero i.e. $S(x) = 0$. The system dynamics during the sliding mode is governed by the switching function. Therefore, $S(x)$ is designed such that a desired dynamics is obtained during the sliding mode.

A suitable switching function is $S(x) = Cx$, where C is defined as $C = [c_1 c_2 1]$. The switching function will be designed if c_1 and c_2 are obtained. The dynamic model of the system during the sliding mode is represented by a reduced system having less number of states than the original model [11]. Using the block diagram of Figure 1, thus a second order (instead of a third order) transfer function can be obtained which models the motor speed deviation in response to load torque during the sliding mode as:

$$\omega_{re}(s) = \frac{-\frac{1}{J}s}{s^2 + \left(\frac{K_m c_2 + f}{J}\right)s - c_1 \frac{K_m}{J}} T_L(s) \quad (2)$$

Equation 2 shows that there is no steady state speed error in response to a step command in T_L . However, the load disturbance rejection capability of the system in transient state is also important. This capability can be increased by the proper selection of vector C . For this purpose 2 can be written in conventional form as:

$$\omega_{re}(s) = \frac{-\frac{1}{J}s}{s^2 + 2\xi\omega_n s + \omega_n^2} T_L(s)$$

where

$$\omega_n^2 = -c_1 \frac{K_m}{J}, \quad 2\xi\omega_n = \frac{K_m c_2 + f}{J} \quad (3)$$

It can be shown that the disturbance rejection depends on natural frequency, ω_n and damping coefficient ξ . Maximum speed deviation in response to load disturbance is reversibly proportional to ω_n . Therefore, it is possible to reduce speed deviation by choosing a large value for ω_n . On the

other hand by increasing ξ it is possible to decrease t_m , the time in which the maximum value of speed deviation occurs. The switching function parameters c_1 and c_2 are given by 4 after selecting proper values for ω_n and ξ as follows:

$$c_1 = -\frac{\omega_n^2 J}{K_m}, \quad c_2 = \frac{2\xi\omega_n J - f}{K_m} \quad (4)$$

Therefore, the switching function $S(x)$ is completely determined.

3.2 Control Signal The system dynamics consists of two modes of operation as mentioned above. Therefore a two-part control signal $u = V_a$ is designed to provide a fast and smooth system dynamics in both modes. The control signal is chosen as:

$$u = V_a = U_1(x) + U_2(x), \quad U_1(x) = Lx, \quad U_2(x) = -\rho \frac{C^T(x)}{|C^T(x)| + \delta}, \quad \rho, \delta > 0 \quad (5)$$

$U_1(x)$ is a linear state feedback control signal where the vector L is defined as:

$$L = [l_1 \ l_2 \ l_3] \quad (6)$$

This part controls the system state trajectory during the reaching mode. The control vector L is designed such that the system state reaches the switching surface with a desired dynamics. L can be calculated by an approach similar to the one presented in [12]. The procedure is not repeated here. However, the results are presented in terms of c_1 and c_2 as follows:

$$\begin{aligned} l_1 &= c_1 La\phi \\ l_2 &= La\left[c_1 + c_2\left(\phi + \frac{f}{J}\right)\right]K_m \\ l_3 &= La\left[\frac{Ra}{La} + \phi - c_2 \frac{K_m}{J}\right] \quad (\phi \text{ is a negative scalar}) \end{aligned} \quad (7)$$

TABLE 1. PMDC Motor Specifications.

Ra	3.2 Ω	La	0.0086 H
f	1.1e-4 Nm/rad/s	J	3e-5 kg.m ²
Km	0.006 v/rad/s	Normal Max. Speed	2100 rpm

TABLE 2. Controller Parameters by Using Different Values for ω_n and ξ .

ξ	ω_n	c_1	c_2	l_1	l_2	l_3
3	15	-1.1250	0.4317	0.7740	-0.2870	1.7695
3	20	-2.0000	0.5817	1.3760	-0.3930	1.5115
4	18	-1.6200	0.7017	1.1146	-0.4686	1.3051
1.2	18	-1.6200	0.1977	1.1146	-0.1377	2.1720

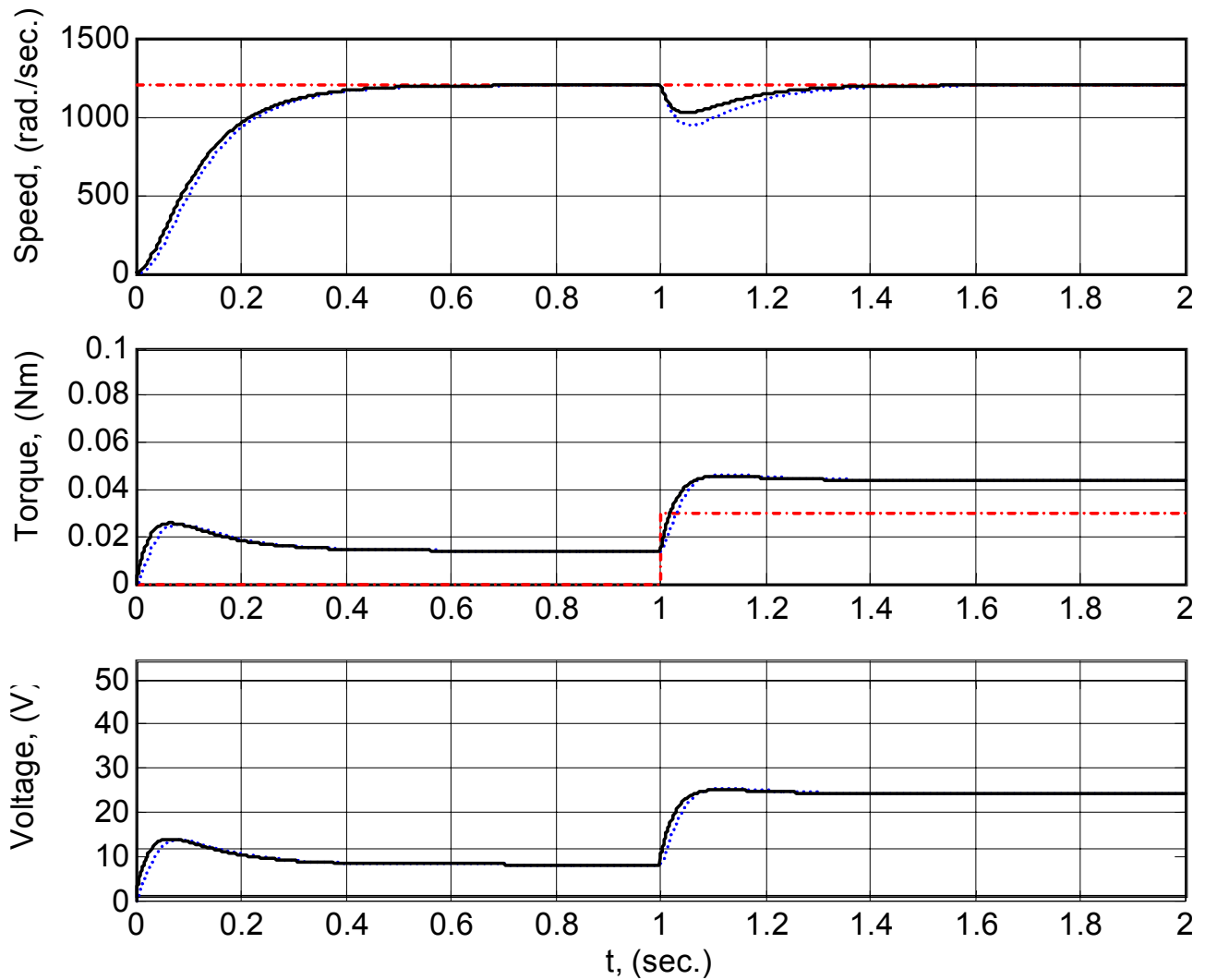


Figure 2. Motor performance under a 0.03 Nm load torque; SMC (solid), FC (dotted).

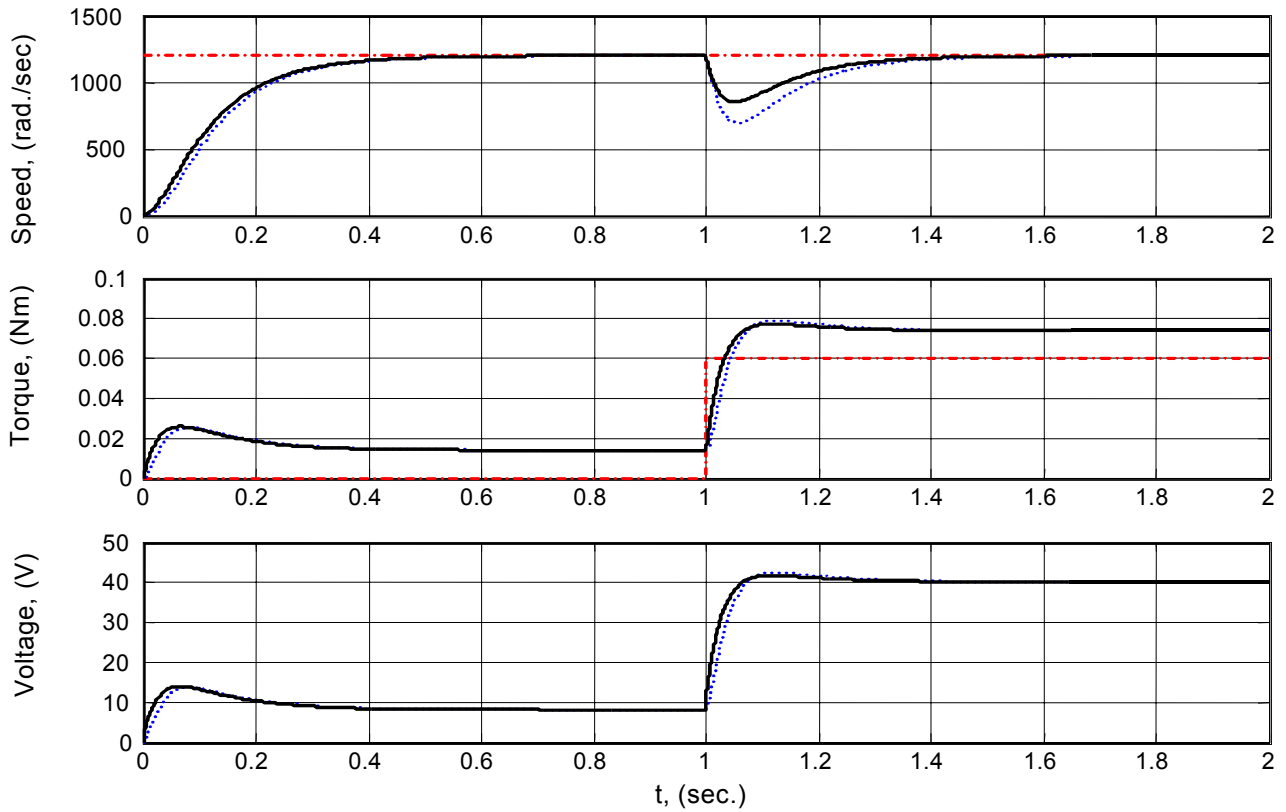


Figure 3. Motor performance under a 0.06 Nm load torque; SMC (solid), SFC (dotted).

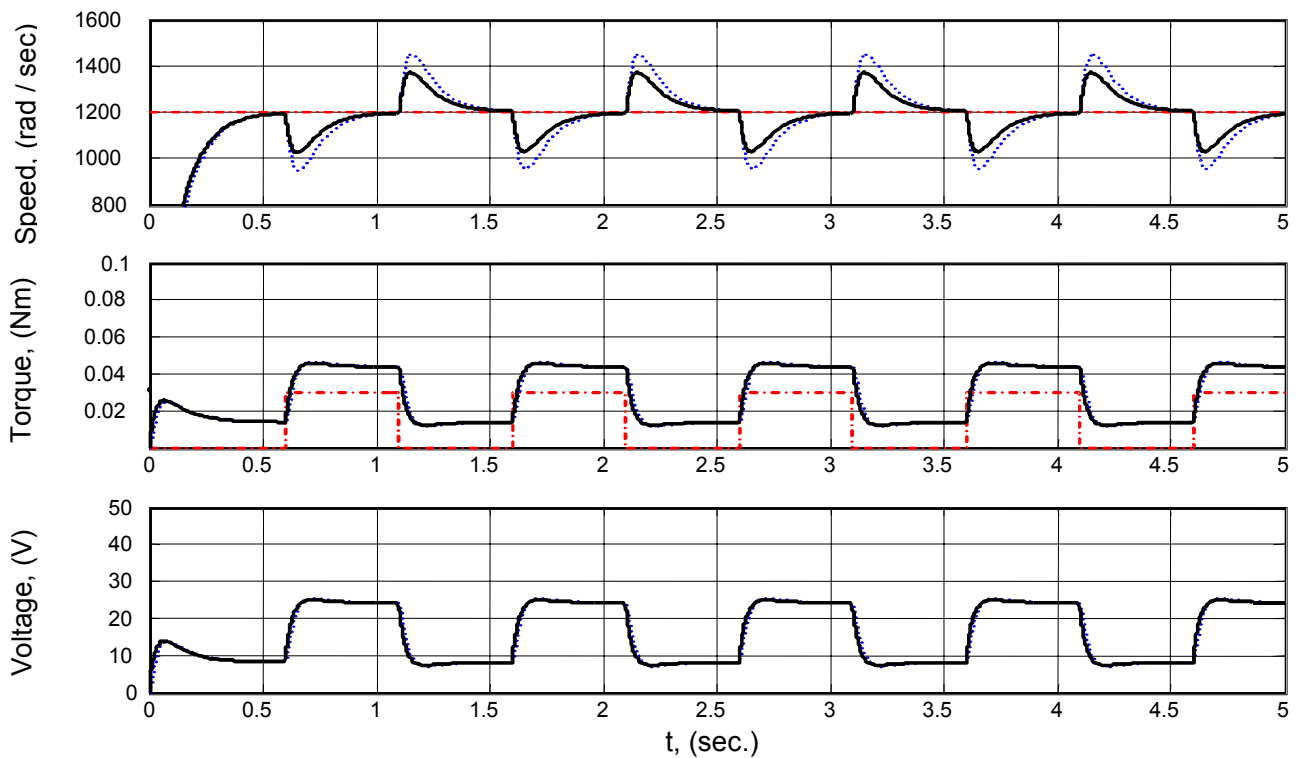


Figure 4. Motor performance under a pulsed torque; SMC (solid), SFC (dotted).

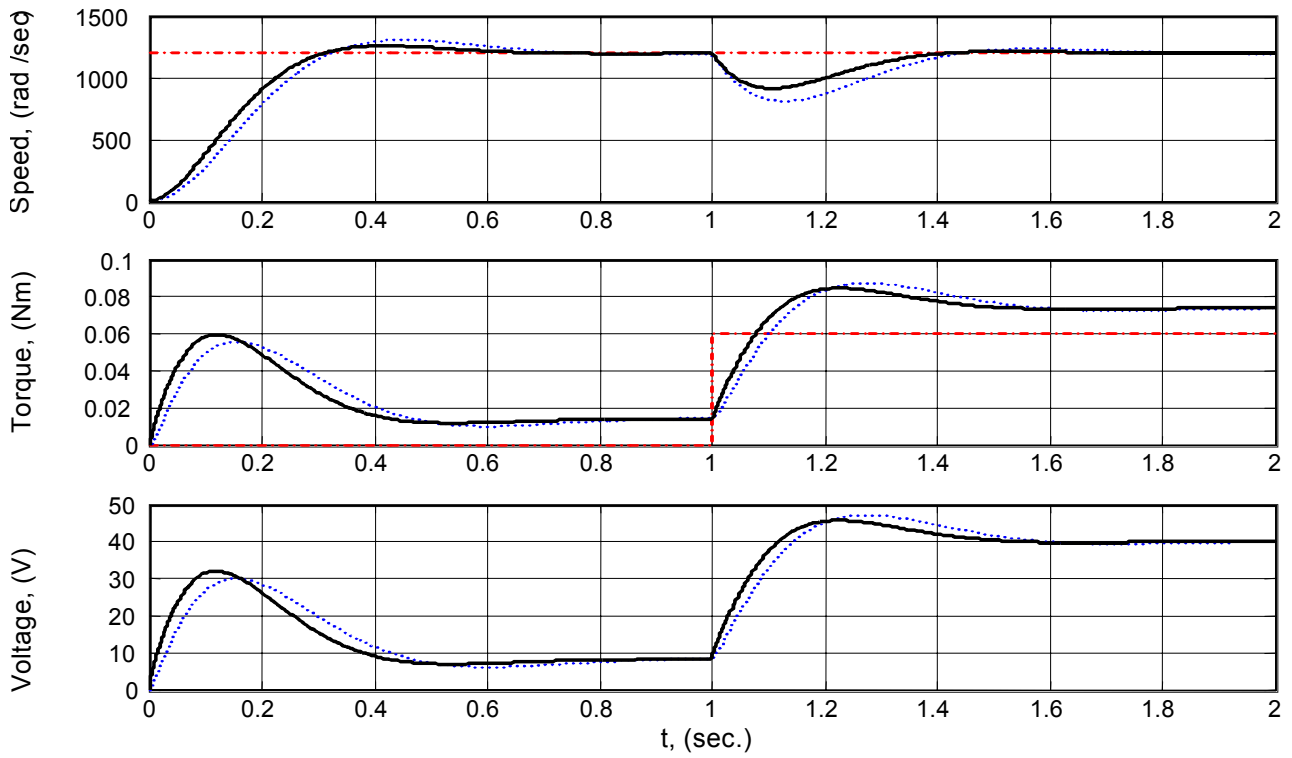


Figure 5. Motor performance with increased inertia coefficient; SMC (solid), SFC (dotted).

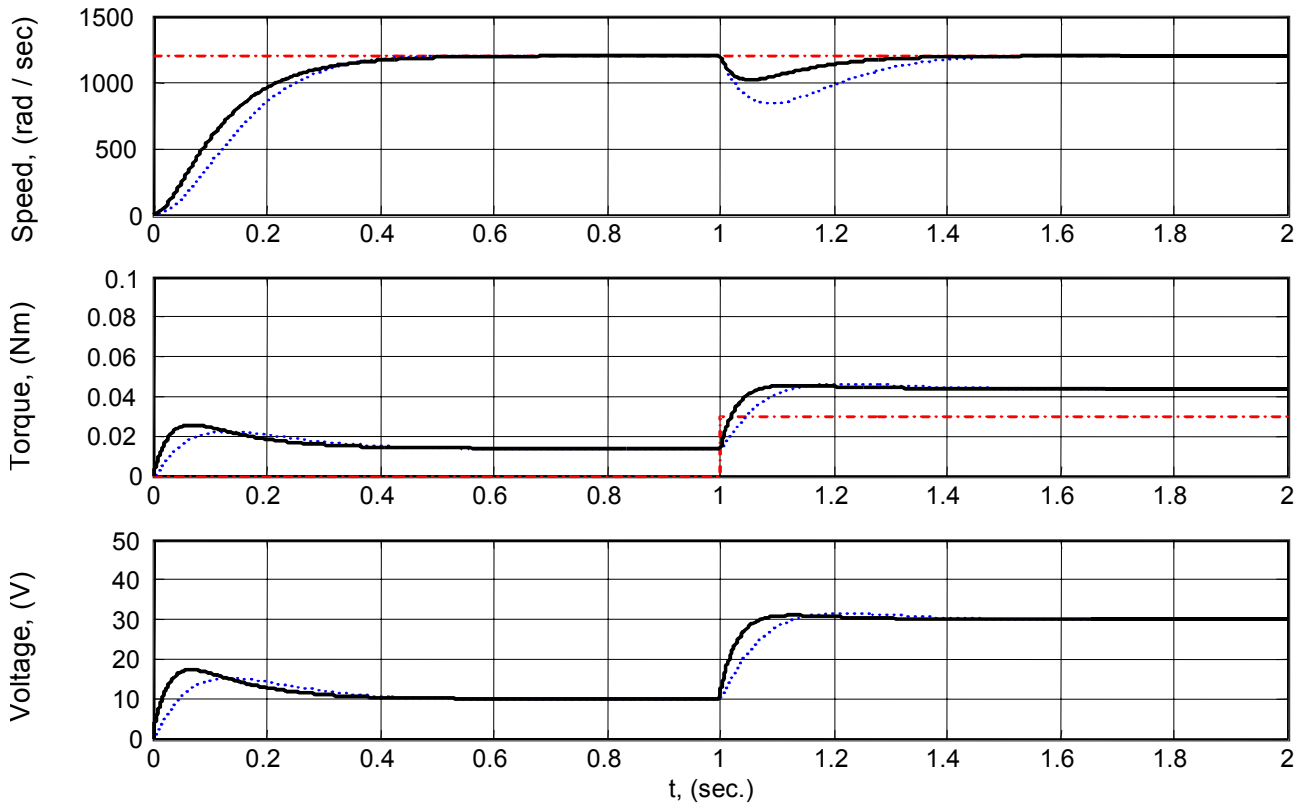


Figure 6. Motor performance with increased stator resistance; SMC (solid), SFC (dotted).

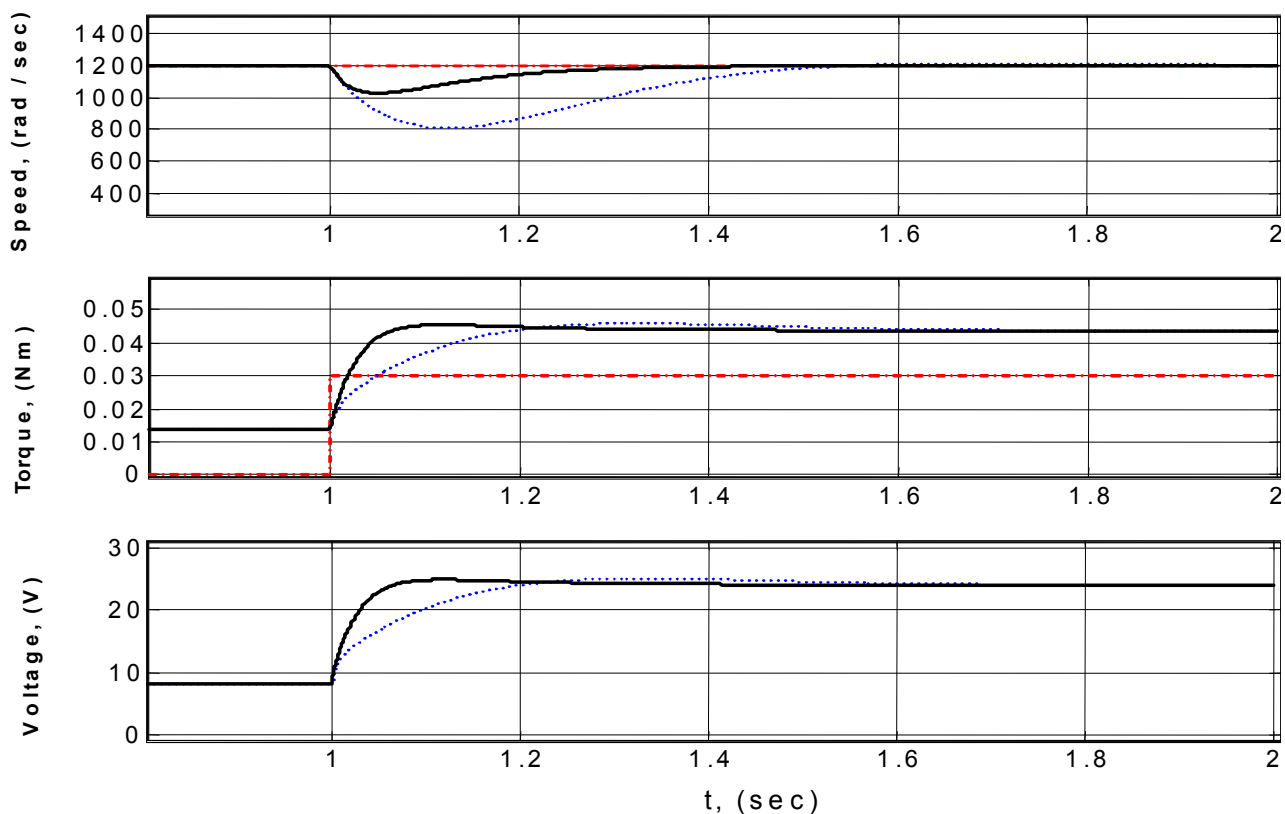


Figure 7. Motor performance under SMC with current signal (solid) and under SMC without current signal (dotted).

$U_2(x)$ is the switching part of the control signal. This part forces the system to remain on the switching surface and slide towards the desired point. A salient feature of the proposed SMC over a conventional SMC is the utilization of the motor current in the control signal as seen in 5. This provides an extra control component that contributes to a stronger control signal. As a result, a faster motor dynamics is obtained. In fact the motor electrical time constant is much smaller than the motor mechanical time constant. Therefore, the current built up is achieved very quickly at the motor start. This current is used in control signal to reduce the speed error. The presence of δ provides a continuous performance and reduces the chattering. Thus a relatively smooth performance is achieved during the switching mode [11]. The value of δ is usually chosen equal to a small real number less than unity. The parameter ρ determines the strength of the switching part with respect to the linear part of the control signal. By choosing $\rho=0$ the sliding mode is completely disappears and the

system robustness against load disturbances and parameter variations fails. On the other hand increasing ρ provides the robustness of the system. However, choosing a very high value for ρ causes a high control effort "u" without substantial improvement in the system robustness. Therefore, a compromise should be made to reach a suitable value of ρ . Repeating the design a few times and looking at the simulation results can easily do this. Different control system designs based on the described approach are carried out for the PMDC motor with specifications listed in Table 1.

By determining different performance specifications for damping and natural frequency, different sets of L and C vectors are obtained as seen in Table 2. The parameters δ and ρ are chosen equal to 0.15 and 12 respectively.

4. SYSTEM SIMULATION

The PMDC motor performance under the sliding

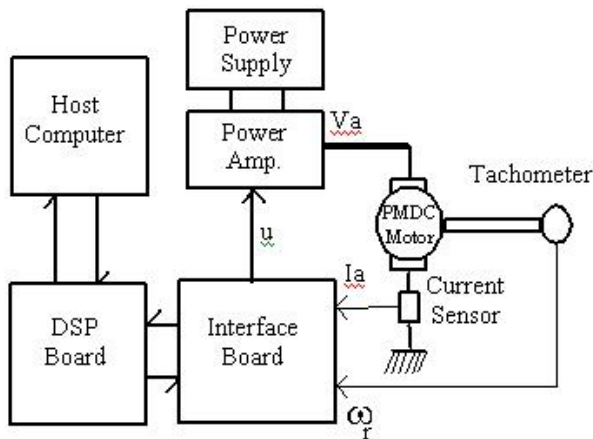


Figure 8. Experimental set-up.

mode controller is examined extensively by computer simulation and the results are presented in Figures 2-5 by solid lines. The control parameters listed in the last row of Table 2 are used in the simulation to achieve a motor speed signal with a relatively short rise time and no or little overshoot. The motor performance under a linear state feedback controller (SFC) without a SMC is also simulated in parallel and its results are plotted in the same Figures by a dotted line for the sake of comparison.

The motor start up at no load and its response to a moderate load torque of 0.03 Nm are shown in Figure 2. It is seen that the proposed SMC in comparison to the SFC provides about %50 less speed deviation when the load is applied. It means that the proposed controller enhance the system performance in terms of robustness. Figure 3 shows similar results but with a saviour load torque of 0.06 Nm. It is seen that the system response to this higher load is deteriorated much more under the SFC than under the SMC. In fact the speed deviation is more than %50 higher with the former. The same conclusion can be drawn from Figure 4 where it shows the system performance in response to a pulsed load torque.

The proposed controller is examined under increased system inertia. The simulation results are shown in Figure 5 where J is three times the rated motor inertia coefficient. It is seen that the proposed SMC performs better than the SFC in terms of motor speed rise time and overshoot at the motor start. It also provides less speed deviation in response to the applied load. The robustness of

SMC against motor parameter variation is also considered by changing the motor stator resistance R_a . Figure 6 shows the motor performance at the same conditions as in Figure 2 except R_a is 4 Ω instead of 3.2 Ω . Comparing Figure 6 to Figure 2, it is seen that the proposed controller is robust against this parameter variation while the SFC is not.

As mentioned before, an advantage of the proposed controller is the presence of the motor current in the control signal. The effect of this feature on the system performance can be seen in Figure 7 where the proposed controller is compared with a controller without the motor current in control signal. It is seen that the use of current signal results in a much faster speed restoration after the load is applied to the machine. This is due to a much faster torque response, which in turn is the result of a rapid voltage increase as seen in Figure 7.

5. IMPLEMENTATION AND EVALUATION

5.1 Experimental Set-Up The system set-up is shown schematically in Figure 8. The set-up includes an experimental PMDC motor, a DC power supply, a power amplifier that supplies the motor, a tachometer, and a current sensor. Also a DSP board with an interface board is used to implement the control system. The control algorithm is implemented on the DSP board. The board is based on a floating point TMS320C31 DSP. The DSP is a fast 50MFLOPS, 25MIPS processor, suitable for heavy real time signal processing and advanced motion control applications. The board also includes an analog interface circuit (AIC), which is responsible for A/D and D/A conversions with an adequate sampling rate. An interface board was also built in house to facilitate the connection of the AIC to the high voltage part of the set-up. The DSP is capable of communicating with a PC through a parallel port. This provides the possibility of developing the control software on the PC and downloading it to the DSP memory. However, the DSP board does all the control functions including sampling and program execution. The input signals to the DSP are the motor speed, and the armature current. The speed is measured by a tachometer attached to the motor shaft. The armature current is obtained through a current sensor. The DSP output

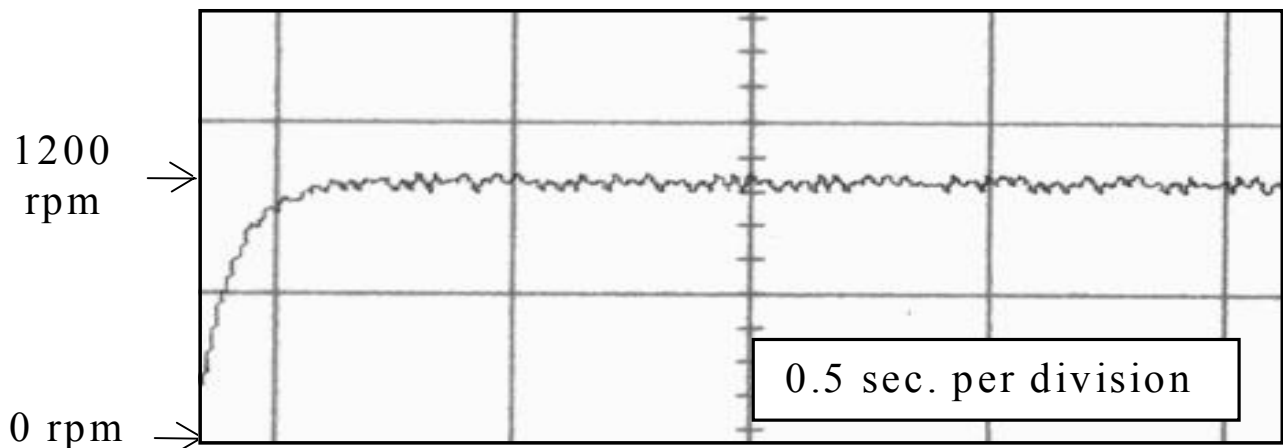


Figure 9. Experimental speed response of motor at start under SMC.

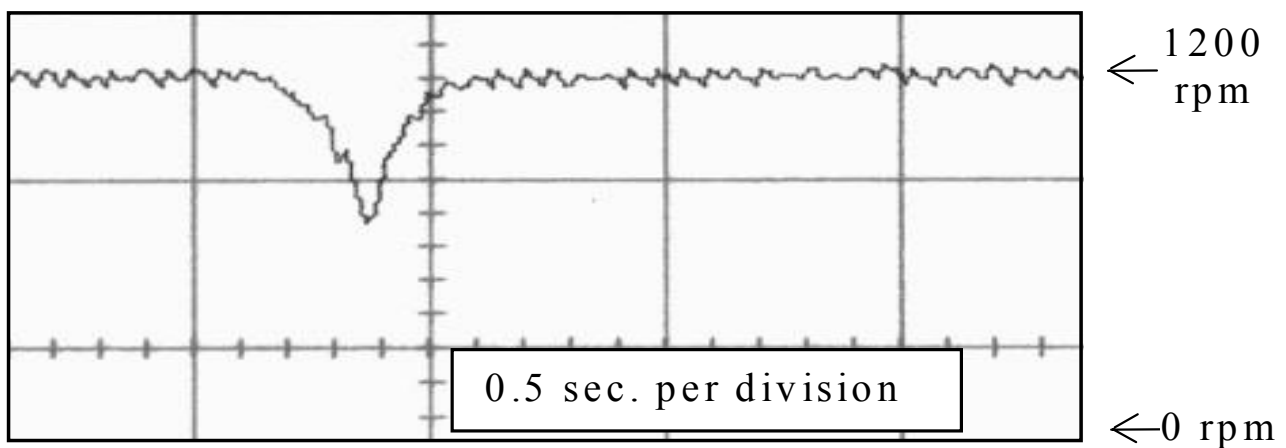


Figure 10. Experimental result of motor load rejection under SMC.

is applied to an amplifier after being isolated and scaled. The amplifier supplies the motor with a variable voltage.

5.2 Experimental Evaluation Using the system set-up described above, different tests are carried out to evaluate the PMDC motor performance under the control system. Figure 9 shows the motor speed during the start. It is seen that a fast and smooth speed signal with no overshoot is achieved. To evaluate the system robustness against external disturbances, applying a relatively heavy load to the motor shaft and monitoring the speed response carry out a load disturbance test. It can be seen in

Figure 10 that the control system is able to restore the original speed after a short dip. These results confirm the simulation results and prove the validity of the proposed controller for high performance PMDC motor drives.

6. CONCLUSIONS

A high performance motor DC control system is presented for permanent magnet DC motors based on sliding mode control theory. The design procedure is described. Special attention is paid to the system robustness under the external disturbances and

parameter variations. The simulation results show desirable motor performance under the proposed controller. An experimental set-up including a low power PMDC motor and a DSP is formed to evaluate the actual motor performance under the proposed control system. The system is evaluated by different tests. The test results show fast and robust motor operation under the presence of the load disturbances and prove validity of the control system.

7. REFERENCES

1. Drury, B., "The Control Techniques Drives and Controls Handbook", *IEE Power Series*, No 35, Cambridge University Press, England, (2001).
2. Utkin, V. I., "Sliding Mode Control Design Principles and Applications to Electric Drives", *IEEE Trans. Ind. Elec.*, Vol. IE-40, No 1, (Feb. 1993), 23-36.
3. Gayed, A., "Time-Domain Simulation of Discrete Sliding Control of Permanent Magnet Synchronous Motors", *Proc. IEEE IECON'95*, Vol. 2, (1995), 754-759.
4. Vaez-Zadeh, S., Bakhtvar, S. M., "Cascade Sliding Mode Control of Permanent Magnet Synchronous Motors", *Proc. IEEE IECON'02*, Spain, (Nov. 2002), 2051-2056.
5. Chern, T. L., Chang, J. and Chang, G. K., "DSP-Based Integral Variable Structure Model Following Control for Brushless DC Motor Drives", *IEEE Trans. on Power Elec.*, Vol. 12, No. 1, (Jan. 1997), 53-63.
6. Baik, I. C., "Robust Non-linear Speed Control of PM Synchronous Motor Using Adaptive and Sliding Mode Control Techniques", *IEE Proc. Electric Power Applications*, Vol. 145, No. 4, (July 1998), 369-376.
7. Brock, S., "Robust Speed and Position Control of PMSM", *Industrial Electronics ISIE '99*, Vol. 2, (1999), 667-672.
8. Bin Zhang, "A PMSM Sliding Mode Control System Based on Model Reference Adaptive Control", *Proc. Power Electronics and Motion Control Conference, PIEMC'00*, Vol. 1, (2000), 336-341.
9. Chern, T. L., Wu, Y. C., "Design of Integral Variable Structure Controller and Application to Electrohydraulic Velocity Servosystems", *IEE Proc. (D)*, 138 (5), (1991), 439-444.
10. Chern, T. L., Wu, Y. C., "Integral Variable Structure Approach for Robot Manipulators", *IEE Proc. (D)*, 139 (2), (1992), 161-166.
11. Slotineand, J. J. E., Li, W., "Applied Nonlinear Control", Englewood Cliffs, NJ, Prentice-Hall, (1991).
12. Zhang, J. and Barton, T. H., "Optimal Sliding Mode Control of Asynchronous Machine Speed with State Feedback", *Conf. Rec. IEEE IAS, Ann. Mtg.*, (1988), 328-333.